the FEBS Journal

Quaternary structure, conformational variability and global motions of phosphoglucosamine mutase

Ritcha Mehra-Chaudhary[1,*], Jacob Mick[1,*], John J. Tanner[1,2] and Lesa J. Beamer[1,2]

1 Biochemistry Department, University of Missouri, Columbia, MO, USA
2 Chemistry Department, University of Missouri, Columbia, MO, USA

Keywords
Bacillus anthracis; negative cooperativity; normal mode analysis; phosphohexomutase; small-angle X-ray scattering

Correspondence
L. J. Beamer, Biochemistry and Chemistry Departments, 117 Schweitzer Hall, University of Missouri, Columbia, MO 65211, USA
Fax: +1 573 884 4812
Tel: +1 573 882 6072
E-mail: beamerl@missouri.edu

*These authors contributed equally to this work

(Received 6 June 2011, revised 11 July 2011, accepted 12 July 2011)

doi:10.1111/j.1742-4658.2011.08246.x

Phosphoglucosamine mutase (PNGM) is a bacterial enzyme that participates in the peptidoglycan biosynthetic pathway. Recent crystal structures of PNGM from two bacterial pathogens, *Bacillus anthracis* and *Francisella tularensis*, have revealed key structural features of this enzyme for the first time. Here, we follow up on several novel findings from the crystallographic studies, including the observation of a structurally conserved interface between polypeptide chains and conformational variability of the C-terminal domain. Small-angle X-ray scattering of *B. anthracis* PNGM shows that this protein is a dimer in solution. Comparisons of the four independent polypeptide chains from the two structures reveals conserved residues and structural changes involved in the conformational variability, as well as a significant rotation of the C-terminal domain, of nearly 60°, between the most divergent conformers. Furthermore, the fluctuation dynamics of PNGM are examined via normal mode analyses. The most mobile region of the protein is its C-terminal domain, consistent with observations from the crystal structures. Large regions of correlated, collective motions are identified exclusively for the dimeric state of the protein, comprising both contiguous and noncontiguous structural domains. The motions observed in the lowest frequency normal mode of the dimer result in dynamically coupled opening and closing of the two active sites. The global motions identified in this study support the importance of the conformational change of PNGM in function, and suggest that the dimeric state of this protein may confer advantages consistent with its evolutionary conservation.

Structured digital abstract
- **PNGM** binds to **PNGM** by x ray scattering (View interaction)

Introduction

The bacterial enzyme phosphoglucosamine mutase (PNGM) participates in the cytoplasmic portion of the peptidoglycan biosynthetic pathway. It catalyzes the interconversion of glucosamine 6-phosphate to glucosamine 1-phosphate, the second step in the production of the key precursor UDP-*N*-acetylglucosamine [1]. Enzymes that participate in the biosynthesis of peptidoglycan are potential targets for antibacterial compounds, as this component of the cell wall is essential for bacteria and absent in humans [2]. Studies of the

Abbreviations
BaPNGM, *Bacillus anthracis* PNGM; D_{max}, maximum particle dimension; FtPNGM, *Francisella tularensis* PNGM; NMA, normal mode analysis; PGM, phosphoglucomutase; PNGM, phosphoglucosamine mutase; R_g, radius of gyration; SAXS, small-angle X-ray scattering.

role of PNGM in a number of human pathogens have shown that the enzyme is important for the viability [3–6] or virulence of bacterial infections [7–11].

Recently, the crystal structures of PNGM from *Bacillus anthracis* [12] and *Francisella tularensis* (J. S. Brunzelle *et al.*, unpublished results) have been determined (Fig. 1). These structures are of considerable interest with regard to inhibitor design efforts for PNGM enzymes. In addition, they provide the first structural description of proteins in the PNGM family, a major subgroup of the large α-D-phosphohexomutase enzyme superfamily [13]. Proteins in the PNGM subgroup have specificity for glucosamine-based phosphosugars, whereas enzymes in the other subgroups of the superfamily utilize glucose, glucose/mannose or *N*-acetylglucosamine-based substrates. Analysis of the *B. anthracis* PNGM (BaPNGM) crystal structure revealed key residues in the active site of the enzyme and a probable role for conformational change in ligand binding and catalysis [12].

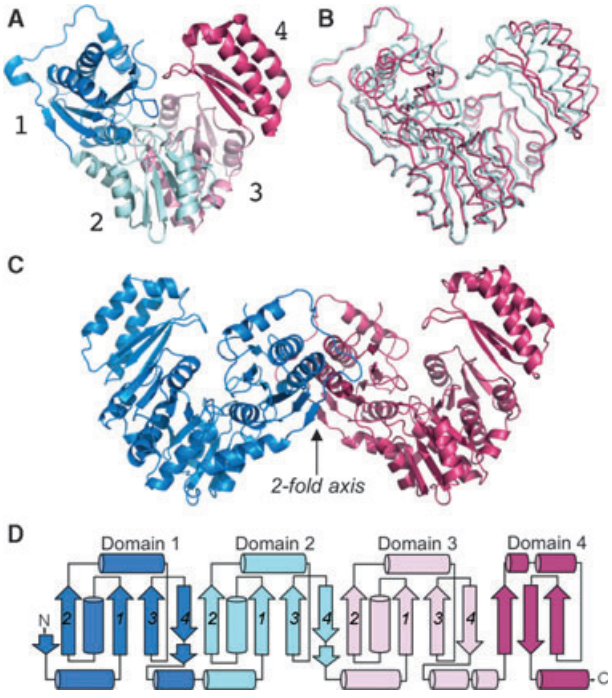

Fig. 1. (A) A ribbon diagram of the protomer of the phosphoglucosamine mutase of *Bacillus anthracis* (BaPNGM) (chain A, closed conformer), showing the four-domain architecture of the protein. Domain 1 (residues 1–152) is shown in blue, domain 2 (residues 153–256) in light cyan, domain 3 (residues 257–369) in pink and domain 4 (residues 370–446) in red. (B) A superposition of the two polypeptide chains in the asymmetric unit of the BaPNGM crystal structure, displaying the variable conformation of domain 4. Chain A is shown in red and chain B in light cyan. (C) The dimer of BaPNGM with one polypeptide chain shown in red and the other in blue. Arrow indicates the two-fold axis. The fully symmetric BaPNGM coordinate set (Materials and methods) was used to produce this figure. (D) A topology diagram of the BaPNGM protomer, colored by domain as in (A). Arrows represent β-strands and cylinders α-helices. Numbers 1–4 indicate the four common β-strands found in the core of domains 1–3, which have similar folding topologies [12].

The crystal structure of BaPNGM (Protein Data Bank ID, 3PDK; UniProt ID, Q81VN7) also revealed a potential dimer interface for the enzyme, the relevance of which was supported by crystal packing analyses and dynamic light-scattering data [12]. A similar interface was noted in the structure of *F. tularensis* PNGM (FtPNGM), despite only moderate sequence identity (39%) between the two proteins. Although sequence identity in the interface is limited, a pattern of conserved residue types at several positions in the interface was identified in multiple sequence alignments [12], raising the possibility that many PNGM proteins may share this oligomeric state.

Here, we describe expanded experimental and computational studies of PNGM, with an emphasis on the characterization of its oligomeric state, the conformational variability of the C-terminal domain and low-frequency motions of the enzyme. Small-angle X-ray scattering (SAXS) demonstrates that BaPNGM exists as a dimer in solution. Structural analyses reveal conserved residues involved in conformational change, and comparisons of four independent polypeptide chains from the two crystal structures highlight a dramatic rotational difference of the C-terminal domain between conformers. Normal mode analyses show that low-frequency fluctuations of the protein are consistent with the conformational variability observed in the crystal structure. The dimer of PNGM exhibits large regions of correlated motion that result in coupled opening and closing of the two active sites. The potential functional implications of these studies are discussed with respect to the evolutionary conservation of the dimer in the PNGM enzyme family.

Results

Quaternary structure

The oligomeric state of PNGM in solution was investigated using SAXS. The experimental scattering curve from SAXS of BaPNGM is shown in Fig. 2A (black curve) and the data are summarized in Table 1. The radius of gyration (R_g), estimated from calculations of the pair distribution function, is 37 Å. For reference, R_g of the dimer in the asymmetric unit of the BaPNGM crystals is 35 Å, whereas R_g of the protomer is only 23 Å. The scattering curve calculated from the

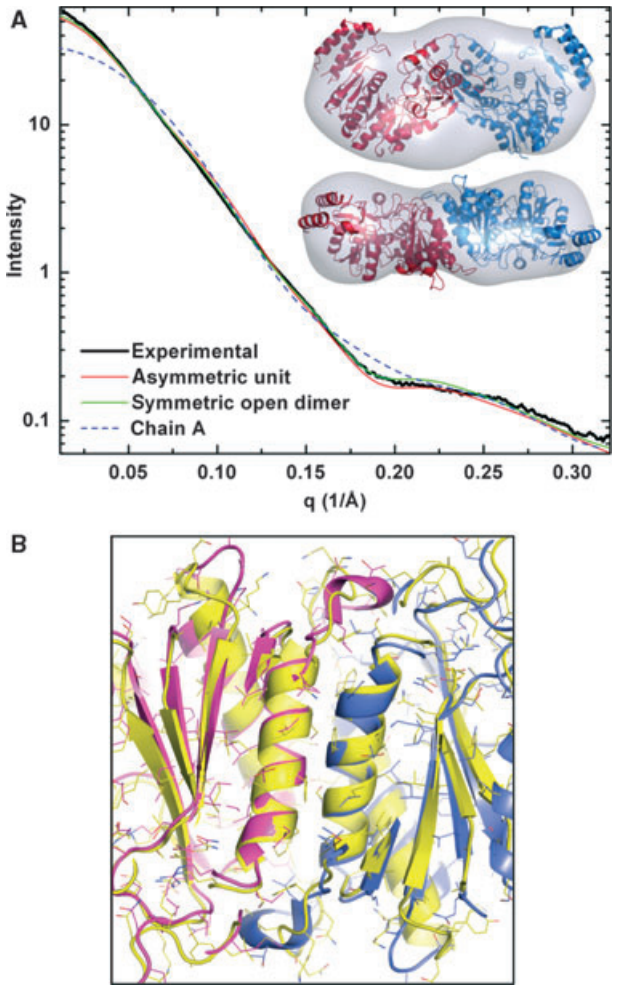

Fig. 2. (A) Small-angle X-ray scattering (SAXS) analysis of the phosphoglucosamine mutase of *Bacillus anthracis* (BaPNGM). The thick full black curve represents the composite experimental scattering curve. The other curves represent SAXS profiles calculated from the dimer of the asymmetric unit (full red), symmetric dimer in which both protomers are in the open state (full green) and chain A of the asymmetric unit (broken blue). The inset shows two orthogonal views of a shape reconstruction calculated using GASBOR assuming two-fold symmetry. The surface represents the SAXS reconstruction (averaged and filtered volume). The structure of the symmetric open dimer of BaPNGM is shown superimposed onto the SAXS shape. Superposition calculations were performed using SUPCOMB [46]. (B) A close-up view showing a superposition of the dimer interface of BaPNGM and *Francisella tularensis* PNGM (FtPNGM). The two chains of BaPNGM are shown as pink and blue ribbons, whereas both chains of FtPNGM are shown in yellow. Side-chains are shown as stick models. The orientation is ~ 90° relative to that in Fig. 1B, parallel to the two-fold axis of the dimer.

dimer in the asymmetric unit exhibits reasonably good agreement with the experimental curve (χ = 7.8, see Fig. 2A). The curve calculated from a dimeric assembly having both protomers in the open state shows better agreement with the experimental profile (χ = 4.2). In contrast, the profile calculated from a BaPNGM protomer is substantially different from the experimental curve (χ = 18.0). These results suggest that BaPNGM exists in solution primarily as a dimer under the conditions used for the SAXS experiments. *Ab initio* shape reconstruction calculations were performed with GASBOR assuming a two-fold symmetric dimer. The normalized spatial discrepancy for the set of 10 GASBOR models is 1.20 ± 0.08, which indicates a reasonably high-quality shape reconstruction. The averaged and filtered volume approximately matches the size and shape of the crystallographic dimer (Fig. 2A, inset). These results suggest that the dimer interface represented by the asymmetric unit is probably formed in solution.

Table 1. Summary of small-angle X-ray scattering (SAXS) analysis.

R_g (Å)[a]	37.18 ± 0.05
D_{max} (Å)[a]	122.0
Normalized spatial discrepancy of GASBOR reconstruction	1.20 ± 0.08
χ from CRYSOL	
Monomer	18.0
Asymmetric unit	7.8
Symmetric dimer	4.2

[a] The real space radius of gyration and maximum particle dimension were estimated from calculations of $P(r)$ using GNOM.

The SAXS data on BaPNGM validate previous crystal packing analyses [12], which indicated that this protein would form a stable dimer in solution. This analysis was conducted by the program PISA [14], which uses thermodynamic calculations to predict the stability of molecular interfaces observed in the crystal lattice. In the case of FtPNGM (Protein Data Bank ID, 3I3W; UniProt ID, Q5NII8), calculations by PISA show an interfacial area of ~ 1130 Å^2 and a complexation significance score of 1.0 (highest possible), predicting that the two chains in the asymmetric unit will also form a stable dimer in solution. A close-up view of the dimer interface on a superposition of the BaPNGM and FtPNGM structures (Fig. 2B) highlights the overall structural similarity of this region. In both proteins, the interface is primarily mediated by contacts between an α-helix in domain 1, with some additional contacts made by residues in nearby loop regions.

To further assess the similarity of the dimer interface in BaPNGM and FtPNGM, we used the program iAlign [15], which was specifically developed for the structural comparison of protein–protein interfaces. Analysis by iAlign shows a total of 47 aligned residues

Table 2. Aligned interface residues in the phosphoglucosamine mutase (PNGM) dimers of *Francisella tularensis* (FtPNGM) and *Bacillus anthracis* (BaPNGM). (:) Amino acid pairs within 5 Å in Cα–Cα distance; (*), identical amino acid pairs. As they are nearly identical, only one of the two possible chain–chain comparisons in the dimer interface is shown. Output from iAlign.

FtPNGM			BaPNGM				
Chain	Residue no.	Residue type	Chain	Residue no.	Residue type	Distance (Å)	Note
A	14	Val	B	13	Val	2.551	:*
A	15	Ala	B	16	Lys	1.530	:
A	20	Thr	B	19	Thr	0.946	:*
A	21	Val	B	20	Pro	0.815	:
A	22	Glu	B	21	Glu	1.030	:*
A	25	Gln	B	24	Phe	0.375	:
A	52	Ser	B	51	Ile	1.080	:
A	53	Ser	B	52	Ser	1.021	:*
A	55	Gly	B	54	His	0.901	:
A	56	Phe	B	55	Met	0.133	:
A	59	Phe	B	58	Gly	0.726	:
A	60	Ala	B	59	Ala	0.469	:*
A	63	Ser	B	62	Ala	0.781	:
A	66	Asn	B	65	Leu	1.374	:
A	67	Ala	B	66	Ser	1.508	:
A	106	Thr	B	105	Gln	1.777	:
A	136	Phe	B	136	Asp	4.791	:
A	138	Tyr	B	140	Arg	2.036	:
A	141	Gln	B	141	Pro	5.070	
A	142	Phe	B	143	Gly	3.120	:
A	143	Lys	B	144	Thr	3.736	:
A	144	Phe	B	146	Leu	1.927	:
A	147	Tyr	B	149	Val	2.761	:
A	209	Leu	B	210	Met	3.216	:

in the interface of the two dimers, with an overall Cα rmsd of 2.2 Å, but a sequence identity of only 19% (notably lower than the overall sequence identity of 39% between the two proteins). Nevertheless, the interface similarity score calculated by iAlign is 0.438 ($P = 3.8 \times 10^{-7}$), consistent with a high level of structural similarity [15,16]. Table 2 lists the aligned residue pairs involved in the interface of the two dimers, which, in both proteins, is a mix of polar and apolar residue types. We note, however, that, of the five residue pairs involved in hydrogen bonds/ion pairs in the BaPNGM dimer [12], none is conserved in the interface of the FtPNGM dimer (data not shown).

Conformational variability of the C-terminal domain

The crystal structure of BaPNGM [12] revealed significant conformational variability in the C-terminal domain of the protein of ~ 30° when comparing the two polypeptide chains in the asymmetric unit (Fig. 1B). Analysis of the conformational differences between these two chains by DynDom allows us to examine the residues and structural changes responsible for the domain 4 rotation of BaPNGM in more detail. We found that the 30° rotation occurs via a hinge-type movement, largely as a result of changes in the backbone angles of residues 367–372, which are at the juncture of domains 3 and 4 of the protein. In BaPNGM, these residues are Thr-Lys-Phe-Pro-Gln-Leu. The backbone angles of residues in this region vary significantly between the two chains in the asymmetric unit, with the largest differences found in ψ of Thr367 (+ 29.5°) and Φ of Gln371 (– 43.6°). Based on a multiple sequence alignment of more than 300 PNGM proteins [12], it can be seen that two of these residues in the hinge region (Pro370 and Gln371) are very highly conserved (98% and 97%, respectively) in this enzyme family.

As is the case with BaPNGM, FtPNGM also crystallizes with two polypeptides in the asymmetric unit, and some conformational variability is also observed between these two chains, although not nearly as much as for BaPNGM. Analysis by DynDom shows that domains 4 of chains A and B of FtPNGM are related by a rotation of ~ 6°, with chain A adopting a slightly more closed conformation with regard to the active site cleft. FtPNGM appears to be one of the few proteins in this family that does not share the conserved Pro and Gln in the interdomain hinge, although generally corresponding residues 367–373 (Gln-Thr-Leu-Ile-Asn-Val) show the largest changes in backbone angles when comparing the two chains in the asymmetric unit. Structural superpositions (data not shown) show that P370 of BaPNGM corresponds to Gln371 of FtPNGM.

Comparisons of the BaPNGM and FtPNGM structures provide additional insights into the conformational flexibility of this enzyme. A superposition of all four crystallographically independent polypeptide chains from the two PNGM structures (Fig. S1A) reveals a continuum of conformers for domain 4. A multiple rmsd plot comparing each pair of the four chains from the two structures versus the residue number (Fig. S1B) shows the overall similarity of the first three domains, and highlights the differences between residues in domain 4. On close examination, the structural superposition shows that, with regard to domain 4, neither chain of FtPNGM aligns well with either chain of BaPNGM. Indeed, when comparing chain B of FtPNGM with chain B of BaPNGM (the two most divergent conformers), analysis by DynDom shows that a 56° rotation of domain 4 is required to

interconvert between the conformers. The significance of this observation is discussed below.

Low-frequency motions

To gain further insights into the conformational variability and dynamic fluctuations of PNGM, we conducted normal mode analysis (NMA) of the protein using elastic network models as implemented by ElNémo [17]. Both the protomer (open conformer, chain A) and the dimer (fully symmetric, see Materials and methods) of BaPNGM were examined in detail. For comparison, the same analyses were conducted for FtPNGM, yielding highly similar results (data not shown), and are therefore not discussed further.

Normal mode calculations for the BaPNGM protomer show that residues in domain 4 of the protein exhibit the largest amplitude fluctuations in the structure, generally moving as a single positively correlated region (Fig. 3A). A large fraction of the conformational variability observed between chains A and B in the crystal structure (Fig. 1B) can be accounted for by the lowest frequency fluctuations of the molecule. Using the Kabsch algorithm [18,19], as implemented in PYMOL [20], an alignment of chains A and B of BaPNGM gives an rmsd of 2.8 Å for all 446 Cα atoms. By applying motions from the lowest frequency normal mode to the coordinates of the open conformer, the Cα rmsd is reduced to 1.1 Å. Some small additional movement from the second normal mode also contributes to the observed conformational change, further reducing the Cα rmsd with the closed conformer to 0.8 Å (Fig. S2).

Normal mode calculations for the dimer of BaPNGM also show that domain 4 of the protein is the most affected by low-frequency normal mode fluctuations (red/yellow regions in Fig. 3B). The overall direction of fluctuation for domain 4 in the dimer is generally similar to that seen in the lowest frequency mode for the protomer. When viewed perpendicular to the long axis of the dimer, it can be seen that the fluctuations associated with this mode describe an overall twisting motion, perpendicular to the long axis of the dimer. Domain 4 of each protomer moves in the opposite direction to its counterpart in the other chain. In contrast, residues involved in the dimer interface, which are essentially all in domain 1 of the protein, exhibit the smallest fluctuations in the structure (dark blue regions in Fig. 3B).

Correlation maps of residue fluctuations from NMA help to visualize groups of residues in PNGM undergoing concerted motions. These are particularly evident in the maps of the dimer, where large groupings

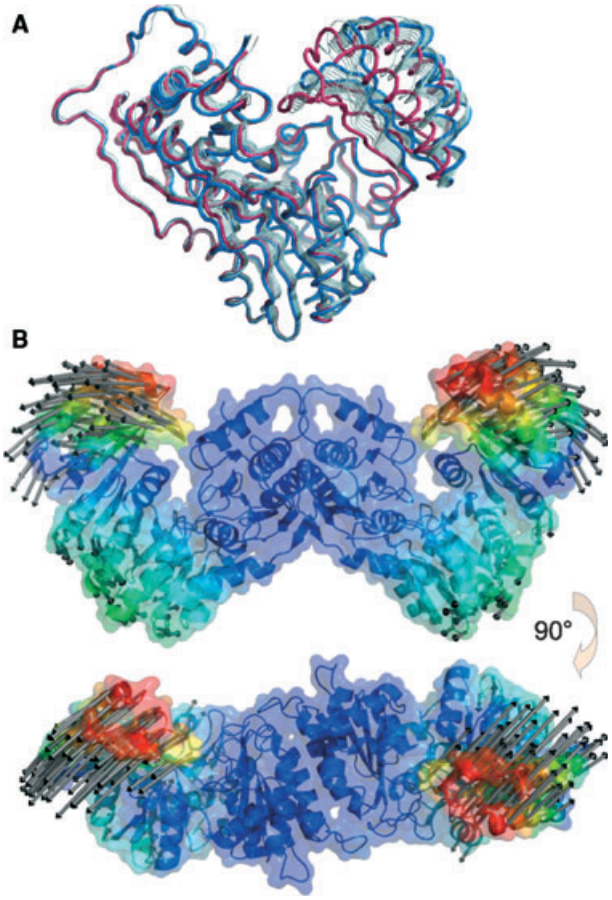

Fig. 3. (A) A superposition of models from the two lowest frequency normal mode fluctuations (thin ribbons, cyan) of the phosphoglucosamine mutase (PNGM) protomer with the two conformers from the crystal structure (open and closed in red and blue, respectively). (B) The *Bacillus anthracis* PNGM (BaPNGM) dimer with vectors indicating the direction of fluctuations for the residues with the largest movements. Orientations are similar to those shown in Fig. 1B. Colors represent the amplitude of vibrations for the first normal mode, with blue being the least motion and red the greatest. The direction of the vectors for domain 4 (red/yellow region with large vectors) is similar to that of domains 1–3 of the alternative monomer (much smaller vectors).

of residues with correlated motions are apparent (Fig. 4A). In this figure, red coloring indicates residues that move in similar directions (positively correlated), whereas blue coloring indicates groups of residues that move in different directions (negatively correlated). The underlying four-domain structure of the protein can be detected in these correlation maps, although it is clear that domains 2 and 3 of each chain of the dimer tend to form a rather large, single unit with positively correlated motions. This domain 2–3 unit of one protomer is negatively correlated with its

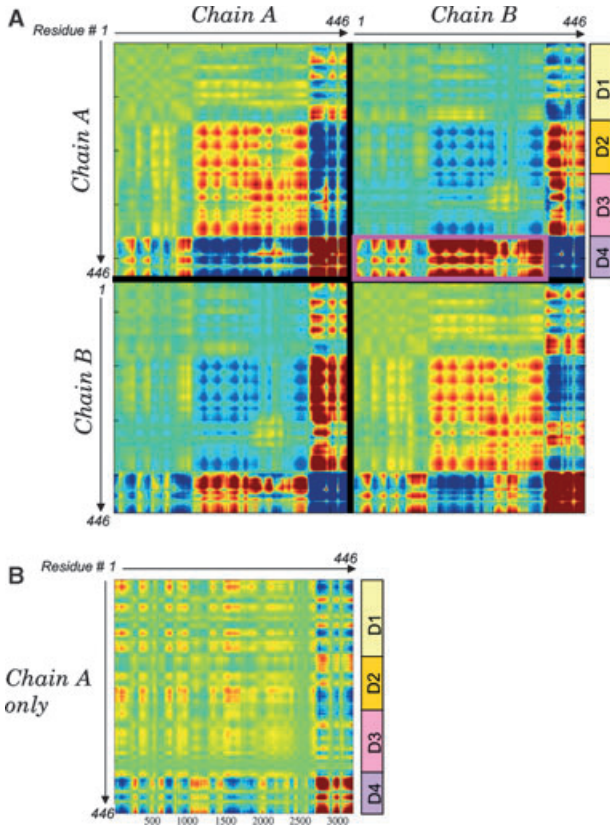

Fig. 4. (A) Correlation maps between residue fluctuations in the *Bacillus anthracis* phosphoglucosamine mutase (BaPNGM) symmetric dimer calculated for the lowest frequency normal mode by ElNémo. Red coloring indicates positively correlated regions, and blue coloring indicates negatively correlated regions. The two axes refer to residue numbers. Black lines separate polypeptide chains; the colored boxes on the right indicate the boundaries of the four protein domains (D1–D4). The pink rectangle in the top right panel highlights the positive correlation between domain 4 of chain A and domains 1–3 of chain B. In the bottom right and top left panels, very small deviations in symmetry between the A and B chains can be seen across the diagonal, presumably as a result of small deviations from perfect symmetry in the Protein Data Bank coordinates. (B) Correlation map for the BaPNGM protomer calculated for the lowest frequency normal mode. Note that the large regions of correlated motions seen in (A) for the dimer are missing in the map for the single chain.

counterpart in the other chain of the dimer. The correlation maps also highlight the fact that the fluctuations of domain 4 of each protomer are negatively correlated with domains 1–3 of the same protomer, but are positively correlated with domains 1–3 from the alternative polypeptide chain (see pink box in Fig. 4A).

Examination of the correlation map of the PNGM protomer (Fig. 4B) shows that it is strikingly different from the corresponding region of the dimer correlation map (top left panel of Fig. 4A). Some hints of negative correlation between domain 4 and the rest of the protein can still be detected, but the domain-sized groupings of positively correlated motions are essentially missing. Instead, smaller clusters of correlated motion are found, in both sequential (along the diagonal) and nonsequential regions of the polypeptide chain.

Discussion

Quaternary structure of the PNGM enzymes and superfamily

The PNGM proteins form a major subgroup of the α-D-phosphohexomutase superfamily. Enzymes in this superfamily participate in a variety of biosynthetic and metabolic pathways, and are present in all kingdoms of life, including bacteria, archaea and eukaryotes [13]. The crystal structures of proteins from the other three major subgroups of the superfamily have revealed a common four-domain architecture for the protomer. Most enzymes in the family studied to date appear to be monomeric [21–23]. However, recent biophysical studies of the phosphoglucomutase (PGM) from *Salmonella typhimurium* have shown that this protein is dimeric [24]. Moreover, a significant subset of bacterial PGMs can be identified as probable dimers based on a highly conserved signature sequence for the dimerization helix.

The SAXS data herein demonstrate that BaPNGM forms a dimer in solution, and support the proposal that the dimer interface observed in the asymmetric unit of BaPNGM and FtPNGM crystals is biologically relevant. Indeed, as these two proteins crystallize in different space groups and have only 39% sequence identity, the observation of a conserved dimer interface is highly correlated with a biologically relevant oligomer [25]. Although no clear dimerization motif is obvious in sequence alignments, a pattern of conserved residue types at several positions of the interface suggests that other PNGM enzymes will share this quaternary structure [12]. The identification of the PNGM dimer, which is structurally distinct from the PGM dimer (data not shown), marks the second subgroup of the α-D-phosphohexomutases with proteins characterized as oligomeric. These results heighten the interest in studies addressing the quaternary structure of other enzymes in the superfamily.

Conformational variability in enzyme function

A role for the conformational flexibility of domain 4 in enzyme function is well substantiated by studies of

other proteins in the α-D-phosphohexomutase superfamily. Typically, binding of the phosphosugar is associated with a hinge-type closure of domain 4, which reduces the volume and surface area of the active site cleft and positions the substrate for phosphoryl transfer. This interdomain rotation is thus critical for both ligand binding and catalysis, as key active site residues are positioned correctly only in the closed conformer of the protein. Because residues involved in catalysis/ligand binding are nearly invariant across the entire superfamily, the closed (ligand-bound) conformer is expected to be highly similar for all proteins, regardless of their subgroup specificity. The crystal structures of enzyme–ligand complexes for other proteins in the superfamily to date support this assertion [22,26]. Similar to BaPNGM, a conserved Pro has been noted in the hinge of the related enzyme *Pseudomonas aeruginosa* phosphomannomutase/PGM, and site-directed mutations of the hinge region of this protein show that the flexibility of the polypeptide backbone is associated with enzyme efficiency [27].

Our comparisons of the four independent polypeptide chains in the BaPNGM and FtPNGM structures show dramatic differences in the orientation of domain 4. Although the comparison of conformers of two different proteins may seem speculative, we note that chain B of BaPNGM adopts a 'closed' conformation that is proposed to closely model the ligand-bound conformer of the enzyme [12]. As FtPGNM shares all of the key active site residues with BaPNGM, it is expected to adopt a nearly identical closed conformation during catalysis, and thus would be required to undergo a rotation of nearly 60°. As neither FtPNGM nor BaPNGM was crystallized with ligand, it seems likely that crystal packing is responsible for the varying conformers observed in these two structures, another indication of the conformational freedom of this domain.

The rotational variability of domain 4 in the two PNGM structures far exceeds that seen for other proteins in the superfamily (typically 10–15°), and even surpasses that noted between the two monomers of BaPNGM (~ 30°). It is possible that the dramatic conformational flexibility of this domain is somehow particularly important for PNGM enzymes (i.e. related to specificity for glucosamine-based substrates), although an explanation of why this might be is not evident. Alternatively, the increased flexibility might be related to the topological differences in domain 4 of PNGM, which has only three β-strands instead of the five strands typically found in enzymes in other subgroups of the superfamily [12]. In either case, this analysis of the PNGM conformers further emphasizes the ubiquity of domain 4 rotation in the α-D-phosphohexomutase superfamily, presumably because of its important functional role in the enzyme reaction.

Functional relevance of correlated movements

The conformational variability of domain 4 observed in the crystal structures of BaPNGM and FtPNGM, and its probable functional significance, prompted our examination of global motions via NMA. In many systems, such analyses have shown that biologically relevant conformational changes of proteins correspond to the lowest frequency vibrational mode(s) of the molecule (for reviews, see [28–30]). NMA of the BaPNGM protomer reveals low-frequency fluctuations that relate to the structural conformers observed in the crystal structure. Domain 4 is found to exhibit global motions that move it in a fashion that reduces the size of the active site cleft and positions residues in domain 4 appropriately for ligand binding. This result is similar to that seen with *S. typhimurium* PGM, where NMA also reproduced varying conformers observed in the crystal structures of the protein [24]. Thus, it appears likely that low-frequency fluctuations of domain 4 are a conserved feature of the entire α-D-phosphohexomutase superfamily, consistent with the similar molecular architecture of these enzymes.

The dimer of BaPNGM was also examined with normal mode calculations. NMA fluctuations are inherently dependent on molecular shape [31], and thus differences in correlated motions between the protomer and dimer are not unexpected. Despite this, we found that domain 4 still undergoes the highest amplitude fluctuations in the structure. However, only in the case of the dimer are large, domain-sized groupings of concerted motions found. Thus, the dimeric structure of the protein appears to be necessary for the long-range effects that produce the correlated motions of these multidomain units. The conservation of the PNGM dimer suggests that its molecular shape may have functional advantages, including, possibly, enhanced collective motions of domains relative to the protomer. These results for the dimer of BaPNGM are similar to those seen for other proteins, including tubulin, where concerted motions of the heterodimer are enhanced relative to those for the individual chains [32], although, in this case, most of the coupled motions were found between sequentially noncontiguous regions.

Are global motions a mechanism for negativity cooperativity?

The low-frequency correlated motions for the PNGM dimer revealed another intriguing feature: dynamically coupled opening/closing of domain 4 in the two polypeptide chains (Figs 3B and S3). This dynamically coupled movement (by which we mean correlated motions that occur simultaneously) produces a dimer in which the two active sites are either both open or both closed at the same time. Similar dynamic coupling has been observed in molecular dynamics simulations of various proteins [33,34]. For the BaPNGM dimer, the coupled movements of domain 4 are intriguing because of the role of this interdomain rotation in enzyme function. More speculatively, they raise the possibility of negative cooperativity for this enzyme.

Negative cooperativity describes the situation in which the affinity of an enzyme for a substrate decreases with an increase in substrate concentration [35]. Although various mechanisms have been proposed, conformational change in response to binding of ligand at one active site, which is then propagated to the other active site rendering it inactive (i.e. ligand-induced conformational change) [36], is a common explanation. The dynamic coupling of the motions described here for BaPNGM suggests that the intrinsic fluctuations of the molecule could provide a mechanism for the propagation of ligand-induced conformational change: as ligand binds to one active site and it begins to close, the other site closes as well, and is thus unavailable for catalysis. A similar rationale has been proposed for the negative cooperativity of ribonuclease A, based on the dynamic coupling observed between subunits [34]. Of course, it is also possible that the dynamically coupled fluctuations of BaPNGM occur in the absence of ligand, which would then be a case of intrinsic allosteric coupling, such as that observed in molecular dynamics simulations of adenylate kinase [33], and consistent with several recent studies of intrinsic dynamics by nuclear magnetic resonance [37].

Additional studies will be needed to assess the significance of global motions in the function of PNGM enzymes and other members of the α-D-phosphohexomutase superfamily. Although, currently, no reports of negative cooperativity can be found in the literature for the PNGMs, this absence of data is inconclusive because of the lack of detailed kinetic studies for these proteins. As a whole, however, these studies suggest an intriguing relationship between functionally important conformational change, global motions and the oligomeric structure of this enzyme family.

Materials and methods

SAXS experiments

BaPNGM protein for these studies was expressed and purified as described previously [38]. SAXS experiments were performed at beamline 12.3.1 of the Advanced Light Source. Prior to analysis, samples of BaPNGM were dialyzed against 50 mM 3-(*N*-morpholino)propanesulfonic acid, pH 7.3, 1 mM $MgCl_2$ and 1 mM tris(hydroxypropyl)phosphine. Scattering intensities (I) were measured at four protein concentrations (2.1, 4.2, 8.4 and 12.5 $mg{\cdot}mL^{-1}$) as a function of the scattering vector $q = (4\pi \sin\theta)/\lambda$, where 2θ is the scattering angle and λ is the wavelength of the incident beam. Exposure times of 0.5, 1.0 and 5.0 s were used. The scattering curves collected from the protein sample were corrected for background scattering using intensity data collected from the dialysis buffer. The composite scattering curve used for shape reconstructions was generated with PRIMUS by scaling and merging the background-corrected high-q region ($q > 0.092$ $Å^{-1}$) data from the highest concentration sample (1.0 s of exposure) with the low-q region ($q < 0.127$ $Å^{-1}$) data from the lowest concentration sample (1.0 s of exposure). Scattering curves were subjected to indirect Fourier transform using GNOM [39] to yield the pair distribution function [$P(r)$], from which the radius of gyration (R_g) and the maximum particle dimension (D_{max}) were estimated. Shape reconstructions were performed using GASBOR [40] with a D_{max} value of 122 Å. Ten independent structural calculations were performed, and the models were averaged and filtered using DAMAVER [41]. Theoretical scattering curves were calculated from atomic coordinates using CRYSOL [42]. MOLEMAN [43] was used to calculate R_g from atomic coordinates.

Normal mode analyses

NMAs were performed using the elastic network model as implemented in the ElNémo server: http://igs-server.cnrs-mrs.fr/elnemo/ [17]. For NMAs, a coordinate set for a fully symmetric dimer of BaPNGM was generated in COOT [44], as the deposited structure (**3PDK**) has variable orientations (open or closed) of the C-terminal domain as a result of crystal packing. A dimer with two open monomers was generated by superimposing monomer A (the open conformer) on residues 1–370 of monomer B (the closed conformer). The open conformer (chain A) was also used for NMA of the BaPNGM protomer. We note that the coarse-grained representation of the protein used for the NMA calculations (one point per residue with connectivity determined solely by distance) does not allow a meaningful analysis starting from the coordinates of the closed conformer of PNGM, as domain 4 is unable to fluctuate because of connections formed with residues in other domains. Moreover, normal modes obtained from the open form of a

protein have been shown to compare better with known conformational changes [45]. The rmsd calculations were performed in PYMOL using the command intra_fit, starting at residue 5 and using only Cα atoms. The correlation plot was produced in MATLAB R2010a (Mathworks, Natick, MA, USA) from the vector output of ElNémo for mode 7. Structural figures were prepared with PYMOL. Vectors in Fig. 3B were made using modevector.py script from the PYMOLWiki website.

Acknowledgements

We thank Cristina Furdui for helpful discussions. This work was supported by a grant from the National Science Foundation (MCB-0918389) to LJB. We thank Dr Greg L. Hura of beamline 12.3.1 for help with SAXS data collection and analysis. Part of this work was performed at the Advanced Light Source, which is supported by the Director, Office of Science, Office of Basic Energy Sciences, of the US Department of Energy under contract DE-AC02-05CH11231.

References

1 Barreteau H, Kovac A, Boniface A, Sova M, Gobec S & Blanot D (2008) Cytoplasmic steps of peptidoglycan biosynthesis. *FEMS Microbiol Rev* **32**, 168–207.
2 Gautam A, Vyas R & Tewari R (in press) Peptidoglycan biosynthesis machinery: a rich source of drug targets. *Crit Rev Biotechnol* doi:10.3109/07388551.2010.525498.
3 De Reuse H, Labigne A & Mengin-Lecreulx D (1997) The *Helicobacter pylori* ureC gene codes for a phosphoglucosamine mutase. *J Bacteriol* **179**, 3488–3493.
4 Mengin-Lecreulx D & van Heijenoort J (1996) Characterization of the essential gene glmM encoding phosphoglucosamine mutase in *Escherichia coli*. *J Biol Chem* **271**, 32–39.
5 Rathi B, Sarangi AN & Trivedi N (2009) Genome subtraction for novel target definition in *Salmonella typhi*. *Bioinformation* **4**, 143–150.
6 Tavares IM, Jolly L, Pompeo F, Leitao JH, Fialho AM, Sa-Correia I & Mengin-Lecreulx D (2000) Identification of the *Pseudomonas aeruginosa* glmM gene, encoding phosphoglucosamine mutase. *J Bacteriol* **182**, 4453–4457.
7 Jolly L, Wu S, van Heijenoort J, de Lencastre H, Mengin-Lecreulx D & Tomasz A (1997) The femR315 gene from *Staphylococcus aureus*, the interruption of which results in reduced methicillin resistance, encodes a phosphoglucosamine mutase. *J Bacteriol* **179**, 5321–5325.
8 Liu XD, Duan J & Guo LH (2009) Role of phosphoglucosamine mutase on virulence properties of *Streptococcus mutans*. *Oral Microbiol Immunol* **24**, 272–277.
9 Shimazu K, Takahashi Y, Uchikawa Y, Shimazu Y, Yajima A, Takashima E, Aoba T & Konishi K (2008) Identification of the *Streptococcus gordonii* glmM gene encoding phosphoglucosamine mutase and its role in bacterial cell morphology, biofilm formation, and sensitivity to antibiotics. *FEMS Immunol Med Microbiol* **53**, 166–177.
10 Wu S, de Lencastre H, Sali A & Tomasz A (1996) A phosphoglucomutase-like gene essential for the optimal expression of methicillin resistance in *Staphylococcus aureus*: molecular cloning and DNA sequencing. *Microb Drug Resist* **2**, 277–286.
11 Yajima A, Takahashi Y, Shimazu K, Urano-Tashiro Y, Uchikawa Y, Karibe H & Konishi K (2009) Contribution of phosphoglucosamine mutase to the resistance of *Streptococcus gordonii* DL1 to polymorphonuclear leukocyte killing. *FEMS Microbiol Lett* **297**, 196–202.
12 Mehra-Chaudhary R, Mick J & Beamer LJ (2011) Crystal structure of phosphoglucosamine mutase from *B. anthracis*, an enzyme in the peptidoglycan biosynthetic pathway. *J Bacteriol* **193**, 4081–4087.
13 Shackelford GS, Regni CA & Beamer LJ (2004) Evolutionary trace analysis of the alpha-D-phosphohexomutase superfamily. *Protein Sci* **13**, 2130–2138.
14 Krissinel E & Henrick K (2007) Inference of macromolecular assemblies from crystalline state. *J Mol Biol* **372**, 774–797.
15 Gao M & Skolnick J (2010) iAlign: a method for the structural comparison of protein–protein interfaces. *Bioinformatics* **26**, 2259–2265.
16 Gao M & Skolnick J (2010) Structural space of protein–protein interfaces is degenerate, close to complete, and highly connected. *Proc Natl Acad Sci USA* **107**, 22517–22522.
17 Suhre K & Sanejouand YH (2004) ElNémo: a normal mode web server for protein movement analysis and the generation of templates for molecular replacement. *Nucleic Acids Res* **32**, W610–W614.
18 Kabsch W (1976) A solution for the best rotation to relate two sets of vectors. *Acta Crystallogr* **32A**, 922–923.
19 Kabsch W (1978) A discussion of the solution for the best rotation to relate two sets of vectors. *Acta Crystallogr* **34A**, 827–828.
20 DeLano WL (2002) *The PyMOL Molecular Graphics System*. DeLano Scientific, San Carlos, CA.
21 Liu Y, Ray W & Baranidharan S (1997) Structure of rabbit muscle phosphoglucomutase refined at 2.4 Å resolution. *Acta Crystallogr D Biol Crystallogr* **53**, 392–405.
22 Nishitani Y, Maruyama D, Nonaka T, Kita A, Fukami TA, Mio T, Yamada-Okabe H, Yamada-Okabe T & Miki K (2006) Crystal structures of N-acetylglucosamine-phosphate mutase, a member of the alpha-D-phosphohexomutase superfamily, and its substrate and product complexes. *J Biol Chem* **281**, 19740–19747.

23 Regni C, Tipton PA & Beamer LJ (2002) Crystal structure of PMM/PGM: an enzyme in the biosynthetic pathway of *P. aeruginosa* virulence factors. *Structure* **10**, 269–279.
24 Mehra-Chaudhary R, Mick J, Tanner JJ, Henzl MT & Beamer LJ (2011) Crystal structure of a bacterial phosphoglucomutase, an enzyme involved in the virulence of multiple human pathogens. *Proteins* **79**, 1215–1229.
25 Xu Q, Canutescu AA, Wang G, Shapovalov M, Obradovic Z & Dunbrack RL Jr (2008) Statistical analysis of interface similarity in crystals of homologous proteins. *J Mol Biol* **381**, 487–507.
26 Regni C, Naught LE, Tipton PA & Beamer LJ (2004) Structural basis of diverse substrate recognition by the enzyme PMM/PGM from *P. aeruginosa*. *Structure* **12**, 55–63.
27 Schramm AM, Mehra-Chaudhary R, Furdui CM & Beamer LJ (2008) Backbone flexibility, conformational change, and catalysis in a phosphohexomutase from *Pseudomonas aeruginosa*. *Biochemistry* **47**, 9154–9162.
28 Bahar I & Rader AJ (2005) Coarse-grained normal mode analysis in structural biology. *Curr Opin Struct Biol* **15**, 586–592.
29 Ma J (2005) Usefulness and limitations of normal mode analysis in modeling dynamics of biomolecular complexes. *Structure* **13**, 373–380.
30 Tama F & Brooks CL (2006) Symmetry, form, and shape: guiding principles for robustness in macromolecular machines. *Annu Rev Biophys Biomol Struct* **35**, 115–133.
31 Lu M & Ma J (2005) The role of shape in determining molecular motions. *Biophys J* **89**, 2395–2401.
32 Keskin O, Durell SR, Bahar I, Jernigan RL & Covell DG (2002) Relating molecular flexibility to function: a case study of tubulin. *Biophys J* **83**, 663–680.
33 Jana B, Adkar BV, Biswas R & Bagchi B (2011) Dynamic coupling between the LID and NMP domain motions in the catalytic conversion of ATP and AMP to ADP by adenylate kinase. *J Chem Phys* **134**, 1035101-1–1035101-10.
34 Merlino A, Vitagliano L, Ceruso MA & Mazzarella L (2004) Dynamic properties of the N-terminal swapped dimer of ribonuclease A. *Biophys J* **86**, 2383–2391.
35 Bisswanger H (2002) *Enzyme Kinetics: Principles and Methods*. Wiley-VCH, Weinheim.
36 Yu EW & Koshland DE Jr (2001) Propagating conformational changes over long (and short) distances in proteins. *Proc Natl Acad Sci USA* **98**, 9517–9520.
37 Henzler-Wildman K & Kern D (2007) Dynamic personalities of proteins. *Nature* **450**, 964–972.
38 Mehra-Chaudhary R, Neace CE & Beamer LJ (2009) Crystallization and initial crystallographic analysis of phosphoglucosamine mutase from *Bacillus anthracis*. *Acta Crystallogr Sect F Struct Biol Cryst Commun* **65**, 733–735.
39 Svergun DI (1992) Determination of the regularization parameter in indirect-transform methods using perceptual criteria. *J Appl Crystallogr* **25**, 495–503.
40 Svergun DI, Petoukhov MV & Koch MH (2001) Determination of domain structure of proteins from X-ray solution scattering. *Biophys J* **80**, 2946–2953.
41 Volkov VV & Svergun DI (2003) Uniqueness of *ab initio* shape determination in small-angle scattering. *J Appl Crystallogr* **36**, 860–864.
42 Svergun D, Barberato C & Koch MHJ (1995) CRYSOL – a program to evaluate X-ray solution scattering of biological macromolecules from atomic coordinates. *J Appl Crystallogr* **28**, 768–773.
43 Kleywegt GJ (1997) Validation of protein models from Calpha coordinates alone. *J Mol Biol* **273**, 371–376.
44 Emsley P & Cowtan K (2004) Coot: model-building tools for molecular graphics. *Acta Crystallogr D Biol Crystallogr* **60**, 2126–2132.
45 Tama F & Sanejouand YH (2001) Conformational change of proteins arising from normal mode calculations. *Protein Eng* **14**, 1–6.
46 Kozin MB & Svergun DI (2001) Automated matching of high- and low-resolution structural models. *J Appl Crystallogr* **34**, 33–41.

Supporting information

The following supplementary material is available:
Fig. S1. (A) A superposition of the four phosphoglucosamine mutase (PNGM) polypeptide chains from the *Bacillus anthracis* (BaPNGM) and *Francisella tularensis* (FtPNGM) crystal structures. (B) Multiple rmsd plot of the four chains in (A).
Fig. S2. A grid showing the rmsd between the closed conformer (chain B) of the *Bacillus anthracis* phosphoglucosamine mutase (BaPNGM) crystal structure (Protein Data Bank ID, **3PDK**) and various models from the two lowest frequency normal mode calculations as calculated by the ElNémo server.
Fig. S3. An animation of the *Bacillus anthracis* phosphoglucosamine mutase (BaPNGM) dimer showing the coupled movements of domain 4 in the two polypeptide chains calculated by normal mode analysis.

This supplementary material can be found in the online version of this article.

Please note: As a service to our authors and readers, this journal provides supporting information supplied by the authors. Such materials are peer-reviewed and may be re-organized for online delivery, but are not copy-edited or typeset. Technical support issues arising from supporting information (other than missing files) should be addressed to the authors.